

Scaling at the OTOC Wavefront: Free versus chaotic models

Jonathon Riddell,¹ Wyatt Kirkby,¹ D. H. J. O’Dell ¹ and Erik S. Sørensen ¹

¹*Department of Physics & Astronomy, McMaster University 1280 Main St. W., Hamilton ON L8S 4M1, Canada.*

(Dated: July 29, 2023)

Out of time ordered correlators (OTOCs) are useful tools for investigating foundational questions such as thermalization in closed quantum systems because they can potentially distinguish between integrable and non-integrable dynamics. Here we discuss the properties of wavefronts of OTOCs by focusing on the region around the main wavefront at $x = v_B t$, where v_B is the butterfly velocity. Using a Heisenberg spin model as an example, we find that the leading edge of a propagating Gaussian with the argument $-m(x)(x - v_B t)^2 + b(x)t$ gives an excellent fit to the region around $x = v_B t$ for both the free and chaotic cases. However, the scaling in these two regimes is very different: in the free case the coefficients $m(x)$ and $b(x)$ have an inverse power law dependence on x whereas in the chaotic case they decay exponentially. We conjecture that this result is universal by using catastrophe theory to show that, on the one hand, the wavefront in the free case has to take the form of an Airy function and its local expansion shows that the power law scaling seen in the numerics holds rigorously, and on the other hand an exponential scaling of the OTOC wavefront must be a signature of nonintegrable dynamics. We find that the crossover between the two regimes is smooth and characterized by an S-shaped curve giving the lifting of Airy nodes as a function of a chaos parameter. This shows that the Airy form is qualitatively stable against weak chaos and consistent with the concept of a quantum Kolmogorov-Arnold-Moser theory.

Introduction: The hallmark of chaos in classical dynamics is an exponential sensitivity to small changes in initial conditions (butterfly effect). This is at odds with quantum mechanics where unitary time evolution means that the overlap between two states is constant in time. Although quantum systems do not display chaos, there are qualitative differences in behavior depending upon whether their classical limit is integrable or nonintegrable (chaotic) [1]. In the latter case we have ‘quantum chaos’ which is well studied in single-particle quantum mechanics, including in experiments [2–12]. On the theoretical side, the main approach has traditionally been through spectral statistics [13, 14]. These have universal properties that depend only on the symmetries of the Hamiltonian and show close agreement with the predictions of random matrix theory (RMT)[15–18]. More recently, attention has shifted to many body quantum chaos and particularly its role in foundational issues such as thermalization in closed quantum systems. One limitation of RMT is that it does not describe thermodynamic quantities like temperature and energy that are needed for such analyzes [19]. This is remedied by the eigenstate thermalization hypothesis (ETH) [20–24] which has been numerically verified in a range of generic models [25–28] but is violated in integrable and localized systems [29–38], as expected. The ETH generalizes RMT and gives identical predictions if one focuses on a small enough region of the spectrum. Any diagnostic of quantum chaos should therefore clearly differentiate between the integrable and ETH cases. While the ETH does give rise to the notion of chaotic eigenstates, it is a time independent statement and does not resemble classical chaos. In fact, aside from the weak ETH (eigenstate typicality) [39–41], it has no classical counterpart.

A truly dynamical diagnostic for quantum many body chaos is provided by out-of-time-ordered correlators (OTOCs) [42–51]. They take the form

$$C(x, t) = \langle [\hat{A}(t), \hat{B}]^\dagger [\hat{A}(t), \hat{B}] \rangle, \quad (1)$$

where \hat{A} and \hat{B} are operators that at $t = 0$ only have local support (act on different individual lattice sites a distance x apart) and hence commute. The average is usually taken over an ensemble diagonal in the energy basis, but some studies have considered pure states as well [52–54]. As \hat{A} evolves in time, it picks up weight throughout the lattice, becoming non-local and causing $C(x, t)$ to become non-zero. This, in effect, tracks the tendency of dynamics to smear information across the system, and it becomes impossible to determine the initial conditions from local data alone. In this respect the OTOC resembles classical chaos where incomplete information leads to exponential inaccuracy. Indeed, the late time value of the OTOC in local spin models does appear to be an indicator of chaos [43, 52–63]. In the classical limit commutators become Poisson brackets which are a diagnostic for classical chaos, and the general expectation is therefore that OTOCs in nonintegrable models experience exponential growth [51],

$$C(0, t) \sim e^{\lambda_L t}, \quad (2)$$

(although we note that integrable systems near unstable points behave similarly [64–69]). The growth is controlled by the quantum Lyapunov exponent λ_L which obeys [51],

$$\lambda_L \leq 2\pi k_B T / \hbar. \quad (3)$$

Models that approach the bound are known as fast scramblers.

An OTOC should also display spatial dependence as information propagates across the system. A recent conjecture gives the *initial* growth of the OTOC wavefront as [70–73]

$$C(x, t) \sim \exp \left[-\lambda_L \frac{(x/v_B - t)^{1+p}}{t^p} \right]. \quad (4)$$

This has been tested in several cases and used to study the many body localization transition [70–82]. When the parameter p , or broadening coefficient, takes the value $p = 0$, Eq. (4) reduces to the simple ‘‘Lyapunov-like’’ exponential growth of

Eq. (2), but for quantum spin models expected to obey ETH it is believed that in general $p > 0$ [70]. However, broadening is not necessarily a general indicator of how close one is to a chaotic model in the sense of ETH [83, 84], and puzzles remain concerning the value of p in this early growth regime. For example, in two dimensions the values of p coincide in chaotic and integrable models, so the broadening coefficient is inadequate for distinguishing them [70], while some studies [70, 72, 85–88] differ on whether the distinction between values of p even exists in either regime.

For interacting models Eq. (4) is usually fitted in regimes where $C(x, t) \ll 1$ [71, 78], corresponding to times well before the arrival of the main front, where $C(x, t)$ is exponentially small and not well suited to experimental or numerical verification, as one requires high accuracy. We instead focus on the main wavefront region around $x = v_B t$ which is the edge of the OTOC “light cone” where $C(x, t) = O(1)$ and show that it carries information about integrability. While there can additionally be signatures of chaos in OTOCs at late times, including long-time oscillations [70, 84, 89–91], it is still preferable to examine the main front because at late times the signal is more likely to suffer contamination from numerical errors or the environment (in the case of experiments).

Recent numerical work in free models has shown that the portion of the OTOC around the wavefront is well-fitted by the *leading edge* of a propagating Gaussian (the peak and trailing edge are not relevant here) [53, 92],

$$C_G(x, t) \sim e^{-m(x)(x-v_B t)^2 + b(x)t}, \quad (5)$$

where $m(x)$ and $b(x)$ have an inverse power law dependence on x . A Gaussian also occurs in random circuit models [83] and wavefront results suggest it would also be found in the critical Ising model [59]. In this paper we point out that in free models the wavefront is an example of a *fold catastrophe*, and this allows us to employ arguments from catastrophe theory, a mathematically rigorous theory of bifurcations. A fold arises where two classical solutions (rays) coalesce and is universally dressed by an Airy wavefunction. Local to the wavefront it can be expanded to give precisely the form in Eq. (5) with power law dependence of $m(x)$ and $b(x)$, thereby analytically verifying the numerics of [53, 92]. However, the converse must also be true: when the scaling disagrees with the catastrophe theory prediction the dynamics must be of a fundamentally different nature to the free case, i.e. nonintegrable (chaotic). We show numerically that the Gaussian wave form of Eq. (5) in fact still holds in the chaotic case but that the scaling of $m(x)$ and $b(x)$ is exponential. We conclude that in locally interacting models the Gaussian wave form Eq. (5) therefore carries signatures of whether the model is free or ETH-obeying.

Model: We consider a Heisenberg spin Hamiltonian with

nearest and next nearest interactions:

$$\begin{aligned} \hat{H}(J_1; \Delta; J_2; \gamma) &= \hat{H}_f + \hat{H}_I \\ \hat{H}_f &= J_1 \sum_{j=1}^{L-1} \left(\hat{S}_j^+ S_{j+1}^- + \text{h.c.} \right) \\ \hat{H}_I &= \Delta \sum_{j=1}^{L-1} \hat{S}_j^Z \hat{S}_{j+1}^Z \\ &+ J_2 \sum_{j=1}^{L-2} \left(\hat{S}_j^+ S_{j+2}^- + \text{h.c.} \right) + \gamma \sum_{j=1}^{L-2} \hat{S}_j^Z \hat{S}_{j+2}^Z, \quad (6) \end{aligned}$$

and open boundary conditions. This model has free, interacting integrable, and interacting non-integrable regimes depending on the choice of the coefficient vector $\vec{c} \equiv (J_1, \Delta, J_2, \gamma)$. We use dimensionless units with $\hbar = k_B = 1$ so that time evolution is generated by the unitary operator $U(t) = e^{-i\hat{H}t}$ and thermal states by the density operator $\rho_\beta = \frac{1}{Z} e^{-\beta\hat{H}}$ where $\hat{H} = \hat{H}(J_1; \Delta; J_2; \gamma)$.

In this work, we focus on two key regimes of our model. The first is the XX chain, $\vec{c}_f = (-0.5, 0, 0, 0)$ which is free. We choose $J_1 = -0.5$ because it sets the butterfly velocity to $v_B = 1$. The second is $\vec{c}_{\text{ETH}} = (-0.5, 1, -0.2, 0.5)$ which has been verified to obey the ETH with periodic boundary conditions [25]. In this latter case we find $v_B > 1$, see the Supplementary Material (SM) [93]. To explore the transition between these limiting regimes we also consider intermediate points for which the interactions are turned on via a tunable parameter $0 \leq \lambda \leq 1$,

$$\hat{H}_\lambda = \hat{H}_f + \lambda \hat{H}_I, \quad (7)$$

such that the variable coefficient vector becomes $\vec{c} = (-0.5, \lambda, -0.2\lambda, 0.5\lambda)$ and smoothly interpolates between \vec{c}_f and \vec{c}_{ETH} .

When considering the free point \vec{c}_f , we use a system size of $L = 1600$, while for the ETH case we use $L = 14$ for the numerics. We leave the investigation of the interacting integrable case to future work. In the free case, the numerics are carried out by exactly diagonalizing the model with a Jordan-Wigner transformation, and dynamically evolving the system via the resulting free fermion Hamiltonian [94]. In the ETH case, the numerics are performed with full spectrum exact diagonalization. We demonstrate that an alternative choice of parameters for \vec{c}_{ETH} leads to the same basic results in the SM [93].

Suitable operators for $\hat{A}(t)$ and \hat{B} must be chosen for the OTOC in Eq. (1). In the ETH regime we use spin operators $\hat{A}(t) = \sigma_1^Z$, and $\hat{B} = \sigma_m^Z$, where x is the distance between sites 1 and m , and the average $\langle \dots \rangle$ is taken over the thermal ensemble restricted to eigenstates with zero magnetization, $m_z = \sum_{j=1}^L \langle \hat{S}_j^Z \rangle = 0$ and inverse temperature $\beta = 1$. In the free case we perform a Jordan-Wigner transformation from spins to fermions, and for simplicity the OTOC we use in this case is

$$C(x, t) = |a_{m,n}(t)|^2 \quad (8)$$

where $a_{m,n}(t) = \{\hat{f}_m^\dagger(t), \hat{f}_n\}$. Here, \hat{f}_m is the annihilation operator for a fermion on site m . Note that if instead of Eq. (8) we use Eq. (1) with operators σ_m^z , then in the case of a pure Gaussian state or a thermal ensemble the dominant dynamical term is in fact $|a_{m,n}(t)|^2$, see Refs. [53, 92] for further details.

Airy light cones in free systems: In 1972 Lieb and Robinson [95] showed that quantum correlations in spin systems propagate at finite speeds and spread out in a light cone-like fashion. Pioneering experiments with ultracold atoms and trapped ions [96–101], where a sudden quench leads to a nonequilibrium state [102, 103], have confirmed this behavior. In particular, the wavefront for interacting bosonic atoms in an optical lattice was measured in experiments to have an Airy function profile [96] in qualitative agreement with theoretical calculations which can be done analytically in certain limits [104]. The associated problem of domain wall propagation [105–112] also yields Airy functions or related kernels for the wavefront. The Airy function shape implies a dynamical scaling behavior, such as a $t^{1/3}$ broadening of the magnetization domain wall in an XX chain [105]. This body of results has led to the notion of an Airy universality class for free systems [113–115].

To explain the ubiquitous presence of Airy functions we use catastrophe theory. Due to topological properties, a *finite set* of bifurcations are structurally stable meaning they are robust to deformations and perturbations and hence occur generically in nature without the need for fine tuning; they are classified by catastrophe theory and form a hierarchy where the higher catastrophes contain the lower ones [116–119]. In optics and hydrodynamics catastrophes appear as *caustics* where the amplitude diverges in the classical limit, with examples including rainbows, gravitational lensing, ship’s wakes and rogue waves [120–124]. Each class of catastrophe is specified by a normal form $\Phi(\mathbf{s}, \mathbf{C})$ which is a polynomial in the state variables $\mathbf{s} = \{s_1, s_2, \dots\}$ that specify the rays and linear in the control parameters $\mathbf{C} = \{C_1, C_2, \dots\}$ that include the coordinates and other parameters. In physical terms $\Phi(\mathbf{s}, \mathbf{C})$ is the action and the local wavefunction is obtained by an elementary path integral over all configurations [125–127]

$$\Psi(\mathbf{C}) = \left(\frac{1}{2\pi}\right)^{n/2} \int_{-\infty}^{\infty} \dots \int d^n s e^{i\Phi(\mathbf{s}; \mathbf{C})}. \quad (9)$$

The simplest in the hierarchy is the fold catastrophe which has one state variable s , one control parameter Z , and a cubic action $\Phi = s^3/3 + Zs$. In this case the wavefunction is directly proportional to the Airy function $\Psi(Z) = \sqrt{2\pi}\text{Ai}(Z)$ which is plotted in Fig. 1(a). The two extrema of $\Phi(s, Z)$ describe the coalescence of two rays as a function of Z . The next catastrophe in the hierarchy is the cusp which has a quartic action (coalescence of three rays) and the wavefunction is known as the Pearcey function [128].

The connection to OTOCs is that in the integrable case where spins map to noninteracting fermions we can show that the edge of a light cone is a catastrophe/caustic where the number of saddles of the action changes, corresponding to

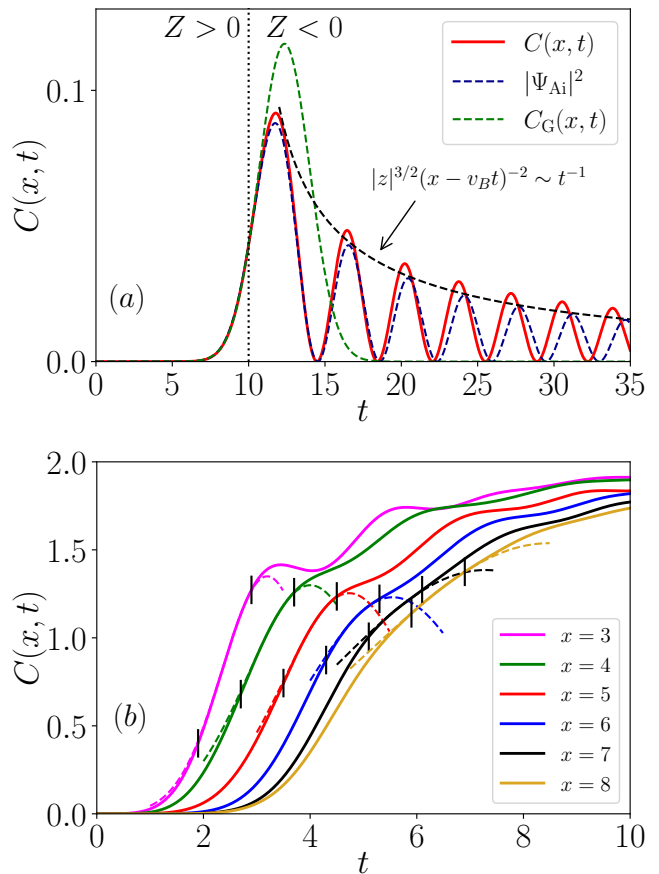


Figure 1. Wavefronts of $C(x, t)$ (a) Free case, \bar{c}_f . Here $x = 10$. Exact numerical results (solid red) along with a fit to the Gaussian form Eq. (5) (green), and the Airy result from Eq. (12) (blue). The expected t^{-1} decay in the amplitude is also shown (black). Note that the part of the wavefront we are fitting to a Gaussian is only a window around $t = 10$. (b) ETH case, \bar{c}_{ETH} , at different positions x . Solid lines indicate the exact OTOC data, and dashed lines are fits to Eq. (5) centered at $x = v_B t$. Vertical bars indicate the fitting window given in Eq. (13).

coalescing quasiparticle trajectories [129]. Consider the case where a quench excites a Bogoliubov fermion at the site at $x = 0$. The resulting wavefunction is [93]

$$\begin{aligned} \Psi(x, t) &= \langle x | e^{-i\hat{H}t} \hat{b}_{x=0}^\dagger | 0 \rangle = \langle x | \sum_k e^{-i\epsilon(k)t} | k \rangle \\ &\approx \frac{\sqrt{a}}{2\pi} \int_{-\pi/a}^{\pi/a} dk e^{i[kx - \epsilon(k)t]} \end{aligned} \quad (10)$$

where a is the lattice constant. The operators \hat{b}_x are the linear combinations of \hat{f}_m and \hat{f}_m^\dagger that diagonalize the Hamiltonian via a Bogoliubov transformation and $\epsilon(k)$ is the Bogoliubov dispersion relation [for the XX chain $\epsilon(k) = 2J_1 \cos ka$]. Putting $\Phi(k, x, t) = kx - \epsilon(k)t$, a caustic occurs at quasi-momentum k_c where two conditions are satisfied [130]

$$(\partial\Phi/\partial k)_{k_c} = 0 \quad \text{and} \quad (\partial^2\Phi/\partial k^2)_{k_c} = 0. \quad (11)$$

The first is Fermat's principle that gives classical rays as saddles of the action $\Phi = \int L dt$ where $L = k\dot{x} - \epsilon(k)$, and the second defines the caustic as the locus of points (x, t) where saddles coalesce. Together, these conditions correspond exactly to the Lieb-Robinson (LR) bound for a light cone as being determined by the maximum value of the group velocity $d\epsilon/dk$ of the fermions [129, 131, 132], $v_{LR} = \max_k |d\epsilon/dk|$.

Why do caustics occur? In classical integrable systems trajectories are confined to live on invariant tori of dimension N in phase space of dimension $2N$, where N is the number of degrees of freedom. Each torus is associated with a family of trajectories that wrap around the torus either periodically or quasiperiodically. When projected down onto coordinate space the edges of the torus lead to a diverging density of trajectories that all have the same position (but different momenta), i.e. a caustic in coordinate space [133].

Identifying light cones in integrable systems as caustics allows rigorous results from catastrophe theory to be applied: **i)** The only structurally stable bifurcations in two dimensions (the space-time formed by x and t) are fold lines that meet at cusp points, as someone who has ironed a shirt knows; **ii)** For a fold catastrophe the phase $\Phi(s, Z)$ is cubic in s ; **iii)** There exists a diffeomorphism from the physical variables (k, x, t) to the canonical Airy cubic form (s, Z) . Therefore, a Taylor expansion truncated at third order about the caustic can give the exact wavefunction in the neighborhood of that point. Adding higher order terms will not affect the qualitative behavior because the merging of two stationary points is fully captured by a cubic action with the tunable parameter Z .

Performing the transformation of variables $s^3 = 2(k - k_c)^3 / [t \partial_k^3 \epsilon(k_c)]$ in Eq. (10) gives [70, 72]

$$\Psi_{\text{Ai}}(x, t) \sim \sqrt{a} \left(\frac{-2}{\partial_k^3 \epsilon(k_c) t} \right)^{1/3} e^{i\Phi(k_c, x, t)} \text{Ai}(Z), \quad (12)$$

where $Z = (x - v_B t) |t \partial_k^3 \epsilon(k_c) / 2|^{-1/3}$ [93]. In Fig. 1(a), we plot $|\Psi_{\text{Ai}}(x, t)|^2$ alongside the numerical result at the point $x = 10$, with the caustic at $Z = 0$ marked by the vertical dotted line. The Airy wavefunction gradually goes out of phase at longer times because the Taylor expansion was made at a single point, but the range could be extended via a uniform mapping onto the tail of a WKB solution [134]. From the asymptotics of the Airy function as $Z \rightarrow -\infty$ it follows that the amplitude of the OTOC decays as $|Z|^{3/2} / (x - vt)^2 \sim 1/t$ inside the light cone (in agreement with Refs. [59, 60]), and the fringe spacing becomes *constant*. Travelling along the wavefront $x/t = v_B$ one finds that the amplitude decays as $x^{-2/3}$ and the width of the primary fringe grows as $t^{1/3}$. Furthermore, Eq. (12) also correctly predicts the early time growth: keeping just the first term of the $Z \rightarrow \infty$ asymptotic series for the Airy function [93] gives the universal $p = 1/2$ form of the OTOC in Eq. (4) [70–72].

Airy functions have been derived for OTOCs before [70, 72, 115]. Our point here is that catastrophe theory guarantees that these results are exact, providing the assumptions underlying Eqns. (10) and (11) hold, namely noninteracting quasipar-

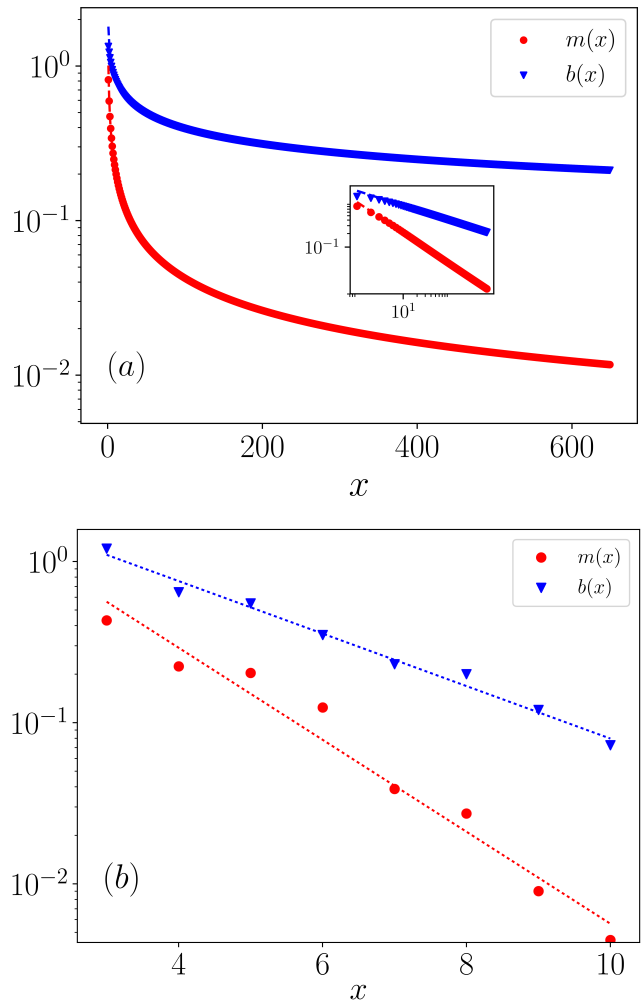


Figure 2. Log-linear plots for the Gaussian parameters $m(x)$ [red] and $b(x)$ [blue]. **(a)** The free Hamiltonian, \bar{c}_f . Dashed lines are fits to Eq. 15. Inset is a log-log plot of the same data. **(b)** The ETH Hamiltonian, \bar{c}_{ETH} , using the same data as in Fig. 1(b) indicating exponential decay of $m(x)$, $b(x)$.

cles with dispersion $\epsilon(k)$. But if these results are exact, any deviation would imply that the assumption of free quasiparticles must be breaking down. We turn to this case below.

The fold is only the first in a hierarchy, and in fact, the two edges of the light cone should generically meet at a cusp. However, the high symmetry of the XX model means that $\epsilon(k)$ is so simple that only two rays can coalesce at once and no cusp occurs, just two pure fold lines that meet at $x = t = 0$. If a symmetry breaking term is added (like in the XY model) three rays can coalesce at the origin and the back-to-back Airy functions are locally replaced by a Pearcey function [129].

Profile of the wavefront in the ETH case: In Fig. 1(b) we plot the exact results for the OTOC for \bar{c}_{ETH} . Fringes are partially visible at smaller x but the Airy nodes have disappeared. At $x = 3$ the wavefront has quite a sharp slope, indicating that the process of scrambling (the increase in non-locality of

the observable) is still in full swing. By $x = 8$, the slope of the OTOC at the wavefront has significantly decreased. The Gaussian waveform of Eq. (5) provides an excellent local fit to the wavefront in both the free [53, 92] and chaotic regimes, as seen from the dashed curves in Fig. 1(a) and 1(b), respectively. The fit is performed over the range

$$t = \frac{x}{v_B} \pm \Delta t, \quad (13)$$

where $\Delta t \approx 0.5$ gives a reasonably large window to describe the shape of $C(x, t)$ at the wavefront. The fits for the parameters $m(x)$ and $b(x)$ in Eq. (5) are shown in Fig. 2 and indicate strong agreement with the data: errors on each term are on the order of 10^{-7} to 10^{-9} for all x . A crucial ingredient to identify the parameters in the ETH case is to first determine the butterfly velocity v_B , which can be done using velocity-dependent Lyapunov exponents [70, 135], as demonstrated in the SM [93]. We find that the velocity for the ETH model characterized by \vec{c}_{ETH} is roughly $v_B \approx 1.28$ (in contrast to $v_B = 1$ for \vec{c}_f). Although the free and ETH wavefronts both display flattening, the scaling properties of $m(x)$ and $b(x)$ are fundamentally different in the two regimes as we now show.

Scaling in Free Models: By expanding the Airy wavefunction given in Eq. (12) about the caustic at $z = 0$ we obtain

$$m(x) = \frac{c_m}{x^{\frac{2}{3}}}, \quad b(x) = \frac{c_b}{x^{\frac{1}{3}}}, \quad (14)$$

where c_m and c_b are constants that depend explicitly on the dispersion relation (see the SM [93] for details). Due to the universality of the Airy wavefunction, this scaling is expected to hold for models which can be written in terms of freely propagating quasiparticles. Furthermore, corrections beyond quadratic order in $x - v_B t$ can be obtained. However, the cubic term in the exponent falls off rapidly (at least as x^{-1}), and so it is reasonable, even at moderate distances, to keep only the Gaussian approximation. We have numerically verified Eq. (14) and the results are shown in Fig. 2(a). Fitting the scaling of each parameter for distances $0 < x \leq 650$ we find,

$$m(x) \propto \frac{1}{x^{a_m}}, \quad b(x) \propto \frac{1}{x^{a_b}}, \quad (15)$$

with $a_m = 0.68857 \pm 0.00008$, and $a_b = 0.33043 \pm 0.00002$, indicating good agreement with the expected values. We also note that because $m(x) \propto b(x)^2$, $m(x)$ falls off significantly quicker than $b(x)$. This may point to an intermediate regime in x where the OTOC is well described by $C(x, t) \sim e^{b(x)t}$.

Scaling in ETH regime: In Fig. 2(b) we show a plot of the data for the \vec{c}_{ETH} case. A linear trend emerges, implying that the spatial dependence on $m(x)$ and $b(x)$ in the ETH regime exhibits exponential rather than power-law decay,

$$b(x) \sim e^{-cx}, \quad m(x) \sim e^{-wx}, \quad (16)$$

where $c, w > 0$ are constants. We find that $c = 0.38 \pm 0.02$ and $w = 0.66 \pm 0.05$. Like the free case, $m(x) \propto b(x)^2$, however, as shown in the SM [93], this is not generally the case.

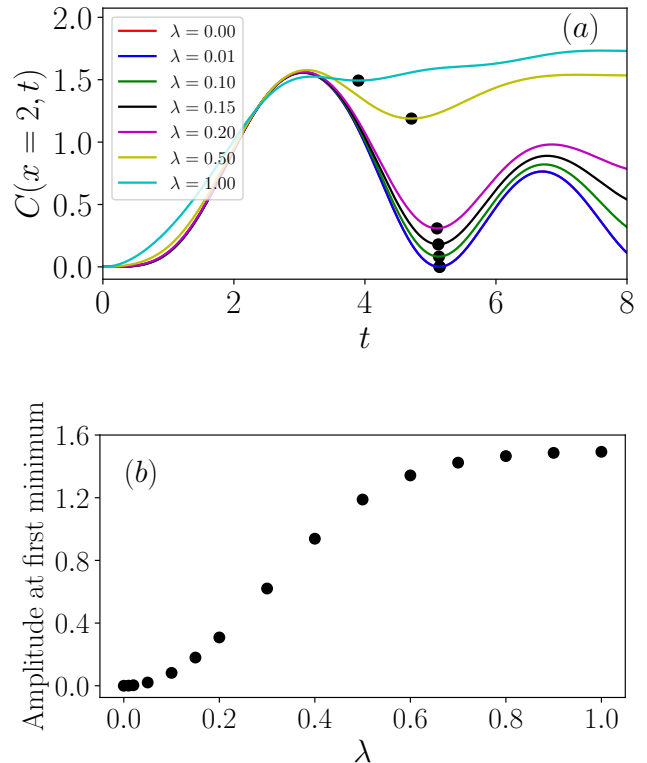


Figure 3. **(a)** Tracking of the first OTOC minimum as a function of time. Interactions are introduced by varying $\vec{c}(\lambda) = (-0.5, \lambda, -0.2\lambda, 0.5\lambda)$, such that $\vec{c}(0) = \vec{c}_f$ and $\vec{c}(1) = \vec{c}_{\text{ETH}}$. Black dots indicate the first minimum after the wave front. **(b)** The height of the first minimum as a function of λ follows an S-shaped curve. The transition to chaos appears to be smooth and the initial lift off is slow indicating that the Airy function solution is qualitatively stable against weak chaos.

The exponentially decaying behavior of $m(x)$ and $b(x)$ is clearly distinct from the free fermion case. This indicates that the Gaussian waveform can distinguish ETH-obeying from free dynamics. In both Figs. 2(a) and (b) $m(x), b(x)$ decay by upwards of two orders of magnitude as a function of position, however the exponential decay in the ETH regime ensures that this occurs over a short distance of $x \approx 10$ while in the free model it takes a distance of $x \approx 600$. Thus, the general flattening of the OTOC at the wavefront (see e.g. Fig. 1) occurs *much* faster in thermalizing models.

Crossover between free and ETH regimes: Fig. 3(a) shows the OTOC as a function of time at the fixed coordinate $x = 2$ for the system described by the tunable Hamiltonian in Eq. (7) for a range of λ . For the free system ($\lambda = 0$), the local minima correspond to Airy zeroes. As λ is increased the integrability is broken and the nodes are lifted up from zero although they remain local minima even in the ETH regime. The amplitude at the first minimum as a function of λ is plotted in Fig. 3(b) and follows a characteristic S-shaped curve

that saturates in the ETH regime. The monotonic increase of this amplitude as a function of λ means that it provides a simple measure of the effect of chaos on the OTOC, and from this point of view it is notable that the lift off is initially slow. A gradual lifting rather than immediate destruction of nodes indicates that the Airy description of the light cone remains approximately correct even in the presence of small integrability-breaking terms. Given the association between caustics and invariant tori in phase space, we are reminded of the Kolmogorov–Arnold–Moser (KAM) theorem that ensures some tori (and therefore caustics) persist for weakly chaotic systems [136]. The survival of the Airy-like form of the wavefront with $\lambda > 0$ is suggestive of the existence of a quantum KAM theory [137–141].

Conclusions: Both numerics and rigorous results based on catastrophe theory show that close to the wavefront free and ETH models can be distinguished by the difference in scaling of the parameters $m(x)$, $b(x)$ in Eq. (5). The ability of modern experiments to realize spin models and measure light cone profiles [96–101] holds out the possibility that this prediction can be tested in the laboratory. Our results also demonstrate the structural stability of the Airy function wavefront against weak chaos. The connection between Airy functions, caustics, and invariant tori in phase space, suggests there is a quantum analogue of the KAM theory [138]. Such a theory would imply that the transition to chaos is smooth and is consistent with the widespread prediction and observation of prethermalized (i.e. nonthermal) phases at short to intermediate timescales after quenches and before full thermalization sets in [142–151].

We acknowledge the support of the Natural Sciences and Engineering Research Council of Canada (NSERC) through Discovery Grants (No. RGPIN-2017-05759 and No. RGPIN-2017-06605). This research was enabled in part by support provided by SHARCNET (sharcnet.ca) and the Digital Research Alliance of Canada (alliancecan.ca).

-
- [1] M. V. Berry, Quantum chaology (The Bakerian Lecture), Proc. R. Soc. A **413**, 183 (1987).
- [2] R. A. Jalabert, H. U. Baranger, and A. D. Stone, Conductance fluctuations in the ballistic regime: A probe of quantum chaos?, Phys. Rev. Lett. **65**, 2442 (1990).
- [3] C. M. Marcus, A. J. Rimberg, R. M. Westervelt, P. F. Hopkins, and A. C. Gossard, Conductance fluctuations and chaotic scattering in ballistic microstructures, Phys. Rev. Lett. **69**, 506 (1992).
- [4] V. Milner, J. L. Hanssen, W. C. Campbell, and M. G. Raizen, Optical billiards for atoms, Phys. Rev. Lett. **86**, 1514 (2001).
- [5] N. Friedman, A. Kaplan, D. Carasso, and N. Davidson, Observation of chaotic and regular dynamics in atom-optics billiards, Phys. Rev. Lett. **86**, 1518 (2001).
- [6] H. J. Stockmann and J. Stein, “Quantum” chaos in billiards studied by microwave absorption, Phys. Rev. Lett. **64**, 2215 (1990).
- [7] S. Sridhar, Experimental observation of scarred eigenfunctions of chaotic microwave cavities, Phys. Rev. Lett. **67**, 785 (1991).
- [8] F. L. Moore, J. C. Robinson, C. Bharucha, P. E. Williams, and M. G. Raizen, Observation of dynamical localization in atomic momentum transfer: A new testing ground for quantum chaos, Phys. Rev. Lett. **73**, 2974 (1994).
- [9] D. A. Steck, W. H. Oskay, and M. G. Raizen, Observation of chaos-assisted tunneling between islands of stability, Science **293**, 274 (2001).
- [10] W. K. Hensinger, H. Häffner, A. Browaeys, N. R. Heckenberg, K. Helmerson, C. McKenzie, G. J. Milburn, W. D. Phillips, S. L. Rolston, H. Rubinsztein-Dunlop, and B. Upcroft, Dynamical tunnelling of ultracold atoms, Nature **412**, 52 (2001).
- [11] S. Chaudhury, A. Smith, B. E. Anderson, S. Ghose, and P. S. Jessen, Quantum signatures of chaos in a kicked top, Nature **461**, 768 (2009).
- [12] Y. S. Weinstein, S. Lloyd, J. Emerson, and D. G. Cory, Experimental implementation of the quantum baker’s map, Phys. Rev. Lett. **89**, 157902 (2002).
- [13] M. C. Gutzwiller, Periodic orbits and classical quantization conditions, J. Math. Phys. **12**, 343 (1971).
- [14] M. V. Berry and M. Tabor, Closed orbits and the regular bound spectrum, Proc. R. Soc. A **349**, 101 (1976).
- [15] E. P. Wigner, On the statistical distribution of the widths and spacings of nuclear resonance levels, Proc. Cambridge Philos. Soc. **47**, 790 (1951).
- [16] C. E. Porter, *Statistical theories of spectra: fluctuations* (Academic Press, New York, 1965).
- [17] M. V. Berry and M. Tabor, Level clustering in the regular spectrum, Proc. R. Soc. A **356**, 375 (1977).
- [18] O. Bohigas, M. J. Giannoni, and C. Schmit, Characterization of chaotic quantum spectra and universality of level fluctuation laws, Phys. Rev. Lett. **52**, 1 (1984).
- [19] L. D’Alessio, Y. Kafri, A. Polkovnikov, and M. Rigol, From quantum chaos and eigenstate thermalization to statistical mechanics and thermodynamics, Advances in Physics **65**, 239 (2016), <https://doi.org/10.1080/00018732.2016.1198134>.
- [20] J. M. Deutsch, Quantum statistical mechanics in a closed system, Phys. Rev. A **43**, 2046 (1991).
- [21] M. Srednicki, Chaos and quantum thermalization, Phys. Rev. E **50**, 888 (1994).
- [22] M. Srednicki, The approach to thermal equilibrium in quantized chaotic systems, Journal of Physics A: Mathematical and General **32**, 1163 (1999).
- [23] M. Rigol, V. Dunjko, and M. Olshanii, Thermalization and its mechanism for generic isolated quantum systems, Nature **452**, 854 (2008).
- [24] G. De Palma, A. Serafini, V. Giovannetti, and M. Cramer, Necessity of eigenstate thermalization, Phys. Rev. Lett. **115**, 220401 (2015).
- [25] T. LeBlond, K. Mallayya, L. Vidmar, and M. Rigol, Entanglement and matrix elements of observables in interacting integrable systems, Phys. Rev. E **100**, 062134 (2019).
- [26] H. Kim, T. N. Ikeda, and D. A. Huse, Testing whether all eigenstates obey the eigenstate thermalization hypothesis, Phys. Rev. E **90**, 052105 (2014).
- [27] R. Mondaini, K. R. Fratus, M. Srednicki, and M. Rigol, Eigenstate thermalization in the two-dimensional transverse field Ising model, Phys. Rev. E **93**, 032104 (2016).
- [28] K. Kaneko, E. Iyoda, and T. Sagawa, Work extraction from a single energy eigenstate, Phys. Rev. E **99**, 032128 (2019).
- [29] G. Biroli, C. Kollath, and A. M. Läuchli, Effect of rare fluctuations on the thermalization of isolated quantum systems, Phys. Rev. Lett. **105**, 250401 (2010).
- [30] H.-H. Lai and K. Yang, Entanglement entropy scaling laws

- and eigenstate typicality in free fermion systems, *Phys. Rev. B* **91**, 081110(R) (2015).
- [31] J. Riddell and M. P. Müller, Generalized eigenstate typicality in translation-invariant quasifree fermionic models, *Phys. Rev. B* **97**, 035129 (2018).
- [32] P. Ribeiro, M. Haque, and A. Lazarides, Strongly interacting bosons in multichromatic potentials supporting mobility edges: Localization, quasi-condensation, and expansion dynamics, *Phys. Rev. A* **87**, 043635 (2013).
- [33] L. Vidmar and M. Rigol, Generalized Gibbs ensemble in integrable lattice models, *Journal of Statistical Mechanics: Theory and Experiment* **2016**, 064007 (2016).
- [34] R. Nandkishore and D. A. Huse, Many-body localization and thermalization in quantum statistical mechanics, *Annual Review of Condensed Matter Physics* **6**, 15 (2015).
- [35] S. Iyer, V. Oganesyan, G. Refael, and D. A. Huse, Many-body localization in a quasiperiodic system, *Phys. Rev. B* **87**, 134202 (2013).
- [36] M. Schreiber, S. S. Hodgman, P. Bordia, H. P. Lüschen, M. H. Fischer, R. Vosk, E. Altman, U. Schneider, and I. Bloch, Observation of many-body localization of interacting fermions in a quasirandom optical lattice, *Science* **349**, 842 (2015).
- [37] H. P. Lüschen, P. Bordia, S. S. Hodgman, M. Schreiber, S. Sarkar, A. J. Daley, M. H. Fischer, E. Altman, I. Bloch, and U. Schneider, Signatures of Many-Body Localization in a Controlled Open Quantum System, *Phys. Rev. X* **7**, 011034 (2017).
- [38] H. P. Lüschen, P. Bordia, S. Scherg, F. Alet, E. Altman, U. Schneider, and I. Bloch, Observation of Slow Dynamics near the Many-Body Localization Transition in One-Dimensional Quasiperiodic Systems, *Phys. Rev. Lett.* **119**, 260401 (2017).
- [39] T. Mori, Weak eigenstate thermalization with large deviation bound (2016), arXiv:1609.09776.
- [40] F. G. S. L. Brandão, E. Crosson, M. B. Şahinoğlu, and J. Bowen, Quantum error correcting codes in eigenstates of translation-invariant spin chains, *Phys. Rev. Lett.* **123**, 110502 (2019).
- [41] A. M. Alhambra, J. Riddell, and L. P. García-Pintos, Time evolution of correlation functions in quantum many-body systems, *Phys. Rev. Lett.* **124**, 110605 (2020).
- [42] B. Yoshida, Firewalls vs. scrambling, *J. High Energ. Phys.* **10**, 132.
- [43] B. Swingle and D. Chowdhury, Slow scrambling in disordered quantum systems, *Phys. Rev. B* **95**, 060201(R) (2017).
- [44] J. R. González Alonso, N. Yunger Halpern, and J. Dreschel, Out-of-time-ordered-correlator quasiprobabilities robustly witness scrambling, *Phys. Rev. Lett.* **122**, 040404 (2019).
- [45] B. Yan, L. Cincio, and W. H. Zurek, Information scrambling and Loschmidt echo, *Phys. Rev. Lett.* **124**, 160603 (2020).
- [46] J. Tuziemski, Out-of-time-ordered correlation functions in open systems: A Feynman-Vernon influence functional approach, *Phys. Rev. A* **100**, 062106 (2019).
- [47] D. Mao, D. Chowdhury, and T. Senthil, Slow scrambling and hidden integrability in a random rotor model, *Phys. Rev. B* **102**, 094306 (2020).
- [48] R. J. Lewis-Swan, A. Safavi-Naini, J. J. Bollinger, and A. M. Rey, Unifying scrambling, thermalization and entanglement through measurement of fidelity out-of-time-order correlators in the Dicke model, *Nat. Commun.* **10**, 1581 (2019).
- [49] S. Nakamura, E. Iyoda, T. Deguchi, and T. Sagawa, Universal scrambling in gapless quantum spin chains, *Phys. Rev. B* **99**, 224305 (2019).
- [50] R. Belyansky, P. Bienias, Y. A. Kharkov, A. V. Gorshkov, and B. Swingle, Minimal model for fast scrambling, *Phys. Rev. Lett.* **125**, 130601 (2020).
- [51] J. Maldacena, S. H. Shenker, and D. Stanford, A bound on chaos, *J. High Energ. Phys.* **2016** (8), 106.
- [52] J. Lee, D. Kim, and D.-H. Kim, Typical growth behavior of the out-of-time-ordered commutator in many-body localized systems, *Phys. Rev. B* **99**, 184202 (2019).
- [53] J. Riddell and E. S. Sørensen, Out-of-time ordered correlators and entanglement growth in the random-field XX spin chain, *Phys. Rev. B* **99**, 054205 (2019).
- [54] X. Chen, T. Zhou, D. A. Huse, and E. Fradkin, Out-of-time-order correlations in many-body localized and thermal phases, *Annalen der Physik* **529**, 1600332 (2017).
- [55] Y. Huang, Y.-L. Zhang, and X. Chen, Out-of-time-ordered correlators in many-body localized systems, *Annalen der Physik* **529**, 1600318 (2017).
- [56] R. Fan, P. Zhang, H. Shen, and H. Zhai, Out-of-time-order correlation for many-body localization, *Science Bulletin* **62**, 707 (2017).
- [57] Y. Chen, Universal logarithmic scrambling in many body localization (2016), arXiv:1608.02765.
- [58] R.-Q. He and Z.-Y. Lu, Characterizing many-body localization by out-of-time-ordered correlation, *Phys. Rev. B* **95**, 054201 (2017).
- [59] C.-J. Lin and O. I. Motrunich, Out-of-time-ordered correlators in a quantum Ising chain, *Phys. Rev. B* **97**, 144304 (2018).
- [60] J. Bao and C. Zhang, Out-of-time-order correlators in the one-dimensional XY model, *Commun. Theor. Phys.* **72**, 085103 (2020).
- [61] D. A. Roberts and B. Yoshida, Chaos and complexity by design, *J. High Energ. Phys.* **2017** (4), 121.
- [62] Y. Huang, F. G. S. L. Brandão, and Y.-L. Zhang, Finite-size scaling of out-of-time-ordered correlators at late times, *Phys. Rev. Lett.* **123**, 010601 (2019).
- [63] M. McGinley, A. Nunnenkamp, and J. Knolle, Slow growth of out-of-time-order correlators and entanglement entropy in integrable disordered systems, *Phys. Rev. Lett.* **122**, 020603 (2019).
- [64] S. Pappalardi, A. Russomanno, B. B. Žunkovic, F. Iemini, A. Silva, and R. Fazio, Scrambling and entanglement spreading in long-range spin chains, *Phys. Rev. B* **98**, 134303 (2018).
- [65] Q. Hummel, B. Geiger, J. D. Urbina, and K. Richter, Reversible quantum information spreading in many-body systems near criticality, *Phys. Rev. Lett.* **123**, 160401 (2019).
- [66] K. Hashimoto, K.-B. Huh, K.-Y. Kim, and R. Watanabe, Exponential growth of out-of-time-order correlator without chaos: inverted harmonic oscillator, *J. High Energ. Phys.* **2020**, 68.
- [67] S. Pilatowsky-Cameo, J. Chávez-Carlos, M. A. Bastarrachea-Magnani, P. Stránský, S. Lerma-Hernández, L. F. Santos, and J. G. Hirsch, Positive quantum Lyapunov exponents in experimental systems with a regular classical limit, *Phys. Rev. E* **101**, 010202(R) (2020).
- [68] T. Xu, T. Scaffidi, and X. Cao, Does scrambling equal chaos?, *Phys. Rev. Lett.* **124**, 140602 (2020).
- [69] W. Kirkby, D. H. J. O'Dell, and J. Mumford, False signals of chaos from quantum probes, *Phys. Rev. A* **104**, 043308 (2021).
- [70] V. Khemani, D. A. Huse, and A. Nahum, Velocity-dependent Lyapunov exponents in many-body quantum, semiclassical, and classical chaos, *Phys. Rev. B* **98**, 144304 (2018).
- [71] S. Xu and B. Swingle, Locality, quantum fluctuations, and scrambling, *Phys. Rev. X* **9**, 031048 (2019).
- [72] S. Xu and B. Swingle, Accessing scrambling using matrix product operators, *Nature Physics* **16**, 199–204 (2019).
- [73] S. Xu, X. Li, Y.-T. Hsu, B. Swingle, and S. Das Sarma, Butter-

- fly effect in interacting Aubry-Andre model: Thermalization, slow scrambling, and many-body localization, *Phys. Rev. Research* **1**, 032039 (2019).
- [74] A. Nahum, S. Vijay, and J. Haah, Operator spreading in random unitary circuits, *Phys. Rev. X* **8**, 021014 (2018).
- [75] C. W. von Keyserlingk, T. Rakovszky, F. Pollmann, and S. L. Sondhi, Operator hydrodynamics, OTOCs, and entanglement growth in systems without conservation laws, *Phys. Rev. X* **8**, 021013 (2018).
- [76] S.-K. Jian and H. Yao, Universal properties of many-body quantum chaos at Gross-Neveu criticality (2018), arXiv:1805.12299.
- [77] Y. Gu, X.-L. Qi, and D. Stanford, Local criticality, diffusion and chaos in generalized Sachdev-Ye-Kitaev models, *J. High Energ. Phys.* **2017** (5), 125.
- [78] S. Sahu, S. Xu, and B. Swingle, Scrambling dynamics across a thermalization-localization quantum phase transition, *Phys. Rev. Lett.* **123**, 165902 (2019).
- [79] T. Rakovszky, F. Pollmann, and C. W. von Keyserlingk, Diffusive hydrodynamics of out-of-time-ordered correlators with charge conservation, *Phys. Rev. X* **8**, 031058 (2018).
- [80] S. H. Shenker and D. Stanford, Black holes and the butterfly effect, *J. High Energ. Phys.* **2014** (3), 67.
- [81] A. A. Patel, D. Chowdhury, S. Sachdev, and B. Swingle, Quantum butterfly effect in weakly interacting diffusive metals, *Phys. Rev. X* **7**, 031047 (2017).
- [82] D. Chowdhury and B. Swingle, Onset of many-body chaos in the $O(N)$ model, *Phys. Rev. D* **96**, 065005 (2017).
- [83] V. Khemani, A. Vishwanath, and D. A. Huse, Operator Spreading and the Emergence of Dissipative Hydrodynamics under Unitary Evolution with Conservation Laws, *Physical Review X* **8**, 031057 (2018).
- [84] N. Anand, G. Styliaris, M. Kumari, and P. Zanardi, Quantum coherence as a signature of chaos, *Phys. Rev. Res.* **3**, 023214 (2021).
- [85] S. Gopalakrishnan, D. A. Huse, V. Khemani, and R. Vasseur, Hydrodynamics of operator spreading and quasiparticle diffusion in interacting integrable systems, *Phys. Rev. B* **98**, 220303(R) (2018).
- [86] P. L. Doussal, S. N. Majumdar, and G. Schehr, Large deviations for the height in 1D Kardar-Parisi-Zhang growth at late times, *EPL (Europhysics Letters)* **113**, 60004 (2016).
- [87] C. Monthus and T. Garel, Probing the tails of the ground-state energy distribution for the directed polymer in a random medium of dimension $d = 1, 2, 3$ via a Monte Carlo procedure in the disorder, *Phys. Rev. E* **74**, 051109 (2006).
- [88] I. V. Kolokolov and S. E. Korshunov, Universal and nonuniversal tails of distribution functions in the directed polymer and Kardar-Parisi-Zhang problems, *Phys. Rev. B* **78**, 024206 (2008).
- [89] E. M. Fortes, I. García-Mata, R. A. Jalabert, and D. A. Wisniacki, Gauging classical and quantum integrability through out-of-time-ordered correlators, *Phys. Rev. E* **100**, 042201 (2019).
- [90] E. M. Fortes, I. García-Mata, R. A. Jalabert, and D. A. Wisniacki, Signatures of quantum chaos transition in short spin chains, *EPL (Europhysics Letters)* **130**, 60001 (2020).
- [91] J. Wang, G. Benenti, G. Casati, and W.-g. Wang, Quantum chaos and the correspondence principle, *Phys. Rev. E* **103**, L030201 (2021).
- [92] J. Riddell and E. S. Sørensen, Out-of-time-order correlations in the quasiperiodic Aubry-André model, *Phys. Rev. B* **101**, 024202 (2020).
- [93] J. Riddell, W. Kirkby, D. H. J. O'Dell, and E. S. Sørensen, Supplementary material (2023).
- [94] P. Coleman, *Introduction to Many-Body Physics* (Cambridge University Press, 2015).
- [95] E. H. Lieb and D. W. Robinson, The finite group velocity of quantum spin systems, *Commun. Math. Phys.* **28**, 251 (1972).
- [96] M. Cheneau, P. Barmettler, D. Poletti, M. Endres, P. Schauß, T. Fukuhara, C. Gross, I. Bloch, C. Kollath, and S. Kuhr, Light-cone-like spreading of correlations in a quantum many-body system, *Nature* **481**, 484–487 (2012).
- [97] T. Fukuhara, P. Schauß, M. Endres, S. Hild, M. Cheneau, I. Bloch, and C. Gross, Microscopic observation of magnon bound states and their dynamics, *Nature* **502**, 76–79 (2013).
- [98] T. Langen, R. Geiger, M. Kuhnert, B. Rauer, and J. Schmiedmayer, Local emergence of thermal correlations in an isolated quantum many-body system, *Nat. Phys.* **9**, 643 (2013).
- [99] P. Jurcevic, B. P. Lanyon, P. Hauke, C. Hempel, P. Zoller, R. Blatt, and C. F. Roos, Quasiparticle engineering and entanglement propagation in a quantum many-body system, *Nature* **511**, 202–205 (2014).
- [100] P. M. Preiss, R. Ma, M. E. Tai, A. Lukin, M. Rispoli, P. Zupanic, Y. Lahini, R. Islam, and M. Greiner, Strongly correlated quantum walks in optical lattices, *Science* **347**, 1229 (2015).
- [101] Y. Takasu, T. Yagami, H. Asaka, Y. Fukushima, K. Nagao, S. Goto, I. Danshita, and Y. Takahashi, Energy redistribution and spatiotemporal evolution of correlations after a sudden quench of the Bose-Hubbard model, *Sci. Adv.* **6**, eaba9255 (2020).
- [102] W. S. Bakr, J. I. Gillen, A. Peng, S. Fölling, and M. Greiner, A quantum gas microscope for detecting single atoms in a hubbard-regime optical lattice, *Nature* **462**, 74–77 (2009).
- [103] C. Weitenberg, M. Endres, J. F. Sherson, M. Cheneau, P. Schauß, T. Fukuhara, I. Bloch, and S. Kuhr, Single-spin addressing in an atomic Mott insulator, *Nature* **471**, 319–324 (2011).
- [104] P. Barmettler, D. Poletti, M. Cheneau, and C. Kollath, Propagation front of correlations in an interacting Bose gas, *Phys. Rev. A* **85**, 053625 (2012).
- [105] V. Hunyadi, Z. Rácz, and L. Sasvári, Dynamic scaling of fronts in the quantum XX chain, *Phys. Rev. E* **69**, 066103 (2004).
- [106] V. Eisler and Z. Rácz, Full counting statistics in a propagating quantum front and random matrix spectra, *Phys. Rev. Lett.* **110**, 060602 (2013).
- [107] V. Eisler and F. Maislinger, Hydrodynamical phase transition for domain-wall melting in the XY chain, *Phys. Rev. B* **98**, 161117(R) (2018).
- [108] V. Eisler and F. Maislinger, Front dynamics in the XY chain after local excitations, *SciPost Physics* **8**, 10.21468/scipostphys.8.3.037 (2020).
- [109] M. Kormos, Inhomogeneous quenches in the transverse field Ising chain: scaling and front dynamics, *SciPost Physics* **3**, 10.21468/scipostphys.3.3.020 (2017).
- [110] V. B. Bulchandani and C. Karrasch, Subdiffusive front scaling in interacting integrable models, *Physical Review B* **99**, 121410(R) (2019).
- [111] J. Viti, J.-M. Stéphan, J. Dubail, and M. Haque, Inhomogeneous quenches in a free fermionic chain: Exact results, *EPL (Europhysics Letters)* **115**, 40011 (2016).
- [112] G. Peretto and A. Gambassi, Ballistic front dynamics after joining two semi-infinite quantum Ising chains, *Physical Review E* **96**, 012138 (2017).
- [113] J.-M. Stéphan, Free fermions at the edge of interacting systems, *SciPost Physics* **6**, 10.21468/scipostphys.6.5.057 (2019).
- [114] M. Fagotti, Higher-order generalized hydrodynamics in one dimension: The noninteracting test, *Physical Review B* **96**,

- 220302(R) (2017).
- [115] B. K. S., D. A. Huse, and M. Kulkarni, Spatiotemporal spread of perturbations in power-law models at low temperatures: Exact results for classical out-of-time-order correlators, *Phys. Rev. E* **104**, 044117 (2021).
- [116] R. Thom, *Structural Stability and Morphogenesis* (Benjamin, Reading MA, 1975).
- [117] V. I. Arnol'd, Critical points of smooth functions and their normal forms, *Russ. Math. Survs.* **30**, 1 (1975).
- [118] T. Poston and I. Stewart, *Catastrophe Theory and Its Applications* (Dover Publications, New York, NY, 2012).
- [119] P. T. Saunders, *An Introduction to Catastrophe Theory* (Cambridge University Press, New York, NY, 1980).
- [120] G. B. Airy, On the intensity of light in the neighbourhood of a caustic, *Trans. Cambridge Philos. Soc.* **6**, 379 (1838).
- [121] J. F. Nye, *Natural Focusing and Fine Structure of Light* (Institute of Physics, Philadelphia, 1999).
- [122] L. Kelvin, Deep water ship-waves, *Philos. Mag.* **9**, 733 (1905).
- [123] R. Höhmann, U. Kuhl, H.-J. Stöckmann, L. Kaplan, and E. J. Heller, Freak waves in the linear regime: A microwave study, *Phys. Rev. Lett.* **104**, 093901 (2010).
- [124] M. Onoratoab, S. Residoric, U. Bortolozzoc, A. Montinad, and F. T. Arecchi, Rogue waves and their generating mechanisms in different physical contexts, *Phys. Rep.* **528**, 47.
- [125] J. J. Duistermaat, Oscillatory integrals, Lagrange immersions and unfolding of singularities, *Commun. Pure App. Math.* **27**, 207 (1974).
- [126] V. Guillemin and S. Sternberg, *Geometric Asymptotics*, Vol. 14 (Am. Math. Soc., Providence, RI, 1977).
- [127] W. Kirkby, Y. Yee, K. Shi, and D. H. J. O'Dell, Caustics in quantum many-body dynamics, *Phys. Rev. Res.* **4**, 013105 (2022).
- [128] T. Pearcey, The structure of an electromagnetic field in the neighbourhood of a cusp of a caustic, *Phil. Mag.* **37**, 311 (1946).
- [129] W. Kirkby, J. Mumford, and D. H. J. O'Dell, Quantum caustics and the hierarchy of light cones in quenched spin chains, *Phys. Rev. Res.* **1**, 033135 (2019).
- [130] M. V. Berry, Singularities in waves and rays, in *Physics of Defects (1980)*, Vol. XXXV, edited by R. Balian and et al. (North-Holland Publishing, Amsterdam, 1981).
- [131] J.-M. Stéphan and J. Dubail, Local quantum quenches in critical one-dimensional systems: entanglement, the Loschmidt echo, and light-cone effects, *J. Stat. Mech.* , P08019 (2011).
- [132] P. Calabrese, F. H. L. Essler, and M. Fagotti, Quantum quench in the transverse field Ising chain: I. time evolution of order parameter correlators, *J. Stat. Mech.* , P07016 (2012).
- [133] M. V. Berry, Semiclassical mechanics of regular and irregular motion, in *Chaotic Behaviour of Deterministic Systems (1981)*, Vol. XXXV, edited by G. Iooss, R. H. G. Helleman, and R. Stora (North-Holland Publishing, Amsterdam, 1983).
- [134] M. V. Berry and K. E. Mount, Semiclassical approximations in wave mechanics, *Rep. Prog. Phys.* **35**, 315 (1972).
- [135] Y.-L. Zhang and V. Khemani, Asymmetric butterfly velocities in 2-local hamiltonians, *SciPost Phys.* **9**, 24 (2020).
- [136] V. I. Arnol'd, *Mathematical Methods of Classical Mechanics* (Springer-Verlag, New York, NY, 1989).
- [137] G. Hose and H. S. Taylor, Quantum Kolmogorov-Arnol'd-Moser-like theorem: Fundamentals of localization in quantum theory, *Phys. Rev. Lett.* **51**, 947 (1983).
- [138] G. Brandino, J.-S. Caux, and R. Konik, Glimmers of a quantum KAM theorem: Insights from quantum quenches in one-dimensional Bose gases, *Phys. Rev. X* **5**, 041043 (2015).
- [139] A. Bastianello, A. De Luca, and R. Vasseur, *J. Stat. Mech.* **2021**, 114003 (2021).
- [140] D. Burgarth, P. Facchi, H. Nakazato, S. Pascazio, and K. Yuasa, Kolmogorov-Arnold-Moser stability for conserved quantities in finite-dimensional quantum systems, *Phys. Rev. Lett.* **126**, 150401 (2021).
- [141] V. B. Bulchandani, D. A. Huse, and S. Gopalakrishnan, Onset of many-body quantum chaos due to breaking integrability, *Phys. Rev. B* **105**, 214308 (2022).
- [142] T. Kinoshita, T. Wenger, and D. S. Weiss, A quantum Newton's cradle, *Nature* **44**, 900 (2006).
- [143] M. Gring, M. Kuhnert, T. Langen, T. Kitagawa, B. Rauer, M. Schreitl, I. Mazets, D. Adu Smith, E. Demler, and J. Schmiedmayer, Relaxation and pre-thermalization in an isolated quantum system, *Science* **337**, 1318 (2012).
- [144] A. Gaunt, R. Fletcher, R. Smith, and Z. Hadzibabic, A superheated Bose-condensed gas, *Nature Phys.* **9**, 271 (2013).
- [145] T. Langen, T. Gasenzer, and J. Schmiedmayer, Prethermalization and universal dynamics in near-integrable quantum systems, *J. Stat. Mech.* **2016**, 064009 (2016).
- [146] B. Bertini, F. H. L. Essler, S. Groha, and N. J. Robinson, Thermalization and light cones in a model with weak integrability breaking, *Phys. Rev. B* **94**, 245117 (2016).
- [147] B. Rauer, S. Erne, T. Schweigler, F. Cataldini, M. Tajik, and J. Schmiedmayer, Recurrences in an isolated quantum many-body system, *Science* **360**, 307 (2018).
- [148] S. Choi, C. J. Turner, H. Pichler, W. W. Ho, A. A. Michailidis, Z. Papić, M. Serbyn, M. D. Lukin, and D. A. Abanin, Emergent SU(2) dynamics and perfect quantum many-body scars, *Phys. Rev. Lett.* **122**, 220603 (2019).
- [149] A. Rubio-Abadal, M. Ippoliti, S. Hollerith, D. Wei, J. Rui, S. L. Sondhi, V. Khemani, C. Gross, and I. Bloch, Floquet prethermalization in a Bose-Hubbard system, *Phys. Rev. X* **10**, 021044 (2020).
- [150] M. Ueda, Quantum equilibration, thermalization and prethermalization in ultracold atoms, *Nat. Rev. Phys.* **2**, 669 (2020).
- [151] D. V. Kurlov, S. Malikis, and V. Gritsev, Quasiconserved quantities in the perturbed spin-1/2 XXX model, *Phys. Rev. B* **105**, 104302 (2022).